

Title: ASSESSING THE COOLING EFFECT OF URBAN TEXTILE SHADING DEVICES THROUGH TIME-LAPSE THERMOGRAPHY

Keywords: *Urban shading; Sun sails; Thermography; Heat mitigation; Street surface temperature*

Abstract: The overheating of the street surfaces has negative impacts on pedestrian comfort and cooling energy consumption. During the past few decades, extensive research has been carried out on heat mitigation technologies. However, there is limited knowledge on the efficacy of textile solar protections at the urban scale. In this paper, we investigate the cooling potential of sun sails on urban surfaces based on field measurements carried out in several streets of Cordoba (Spain). To this end, we develop a novel method based on time-lapse thermography at street level that allows for assessing the thermal behavior of urban scenes, in a comprehensive and agile way. Results show that high-mounted sun sails have a global cooling effect over the street, regardless of its orientation. Decreases due to sun sails in ground temperature reach up to 16°C, and in façade temperature, up to 6°C. Our observations demonstrate that sun sails can provide a heat mitigation efficacy similar to standard technologies while entailing softer levels of intervention.

17 1. Introduction

18 The understanding of the mechanisms that drive urban surface temperature is crucial for sustainable
19 urban planning. Surface overheating has negative impacts on human comfort and city energy
20 consumption [1]. As global warming progresses, heat mitigation has become a top priority for urban
21 planners [2–4]. During the past few decades, intense research has been carried out regarding the
22 efficacy of the different cooling technologies [5,6], and numerous projects have been implemented to
23 cool cities [7,8]. Both simulations and experimental studies have demonstrated that one of the most
24 effective strategies to avoid surface overheating is shading [6,7]. At the urban scale, there are three
25 main ways to achieve this goal: occluded urban morphologies, vegetation, and artificial shading
26 devices. The existing literature mainly focuses on the effects of self-shading urban geometries [9–11]
27 and shade trees [12–14]. In contrast, the attention given to artificial solar protections has been far
28 more limited [15].

29 Textile shading devices are an attractive option when the use of vegetation is restricted, removable
30 solar protections are advisable, or a flexible geometrical design is needed [16]. Mediterranean cities,
31 typically facing these constraints, provide a traditional example of the use of textile solar protections
32 [2,17]. These devices usually consist of a set of sun sails placed as a canopy at different heights within
33 the street canyon (Figure 1).



Fig. 1. Spanish streets with textile canopy shadings known as ‘toldos’ in (from left to right): Trapería St (Murcia, 1905), Sierpes St. (Sevilla, 1918), Preciados St. and Arenal St. (Madrid, 2018).

37 The most evident effect of sun sails is a reduction in the solar radiation penetrating the urban canyon.
38 However, the installation of these devices modifies the street microclimate in other ways, involving
39 changes not only in the radiative fluxes but also in the air temperature and wind flow within the
40 canyon. All these processes affect the energy balance of urban surfaces, and thus their temperature.
41 Up to now, investigations about sun sails have mainly focused on pedestrian comfort [6,15,18–20],
42 leaving their effects on the urban surfaces almost unexplored. This paper aims at filling this gap from
43 an experimental approach by collecting field data on the surface temperature within streets sheltered
44 by sun sails.

45 Measuring surface temperatures within urban canyons constitutes a complex task due to the
46 remarkable variations of this parameter in both time and space [1]. The presence of sun sails over the
47 street brings new research challenges from the methodological point of view. To date, the two most
48 common techniques for measuring surface temperatures at the street scale are [5,21]: contact
49 thermometers [11] and aerial infrared thermography, whether from aircraft [22] or elevated platforms
50 [23]. Both approaches have shortcomings for a comprehensive evaluation of sun sail effects, which
51 requires visualizing the distribution of surface temperatures over all the street facets and the solar
52 sails simultaneously, at different times of the day.

53 The main goal of this work is to assess the potential of sun sails to limit the overheating of street
54 surfaces. We conducted field measurements in four streets of Cordoba (Spain), a Mediterranean city
55 with severe summer conditions, and a long tradition in the use of urban sun sails. To this end, we
56 developed a novel method based on time-lapse thermography at the street level. Infrared images are
57 shot in perspective to frame all the street surfaces in a single picture and repeated several times a day
58 to create a sequence [24]. Measurements took place in streets with two orientations, sheltered by sun
59 sails with different tissue properties. Based on the comparison of results among the cases, we provide
60 guidelines for the installation of street sun sails.

61

62 2. Case study description

63 2.1. City context

64 Cordoba is a mid-sized city located in the south of Spain (37°N). Its historical center has a compact
65 morphology, with deep and intricate street canyons bounded by buildings of unequal heights. The
66 configuration of this urban fabric dates from the Medieval Muslim period of the city and constitutes
67 one of the tourist attractions of the city.

68 Cordoba has a temperate Mediterranean climate, with mild winters and hot and dry summers (Csa,
69 according to Köppen's classification). Long-term records for the region are available from the airport
70 meteorological station, located at a semi-rural location 6 km away from the city center (Table 1).
71 According to this data, mean monthly temperatures (T_{air}) range between 9.3°C in January to 28.0°C in
72 July and August. The annual precipitation level in Cordoba is low, and the number of cloudless days
73 (SD), high, especially in summer. Air temperatures during this season are especially high, with average
74 maximums ($T_{\text{air MAX}}$) ranging from 31°C to 37°C between June and September. Peaks on air
75 temperatures over 40°C and heat waves are recurrent in these months. Normal wind conditions on
76 the outskirts of Cordoba are light breezes, lower than 3 m/s on average [25]. Due to urban
77 obstructions, episodes with no wind are frequent within the city, especially at the bottom of deep
78 urban canyons. These severe climatic conditions represent a source of discomfort not only for the
79 citizens but also for tourist visitors, limiting the number and intensity of activities held outdoors in the
80 summertime.

81

82
83

Table 1. Cordoba Climate (Source: data between 1981-2005 at the Airport – AEMET Service) [25]

	Tair _{MAX} (°C)	Tair (°C)	Tair _{MIN} (°C)	RH (%)	SD	I (h)
Jan	14,9	9,3	3,6	76	10,3	174
Feb	17,4	11,1	4,9	71	8,8	186
Mar	21,3	14,4	7,4	64	8,5	218
Apr	22,8	16,0	9,3	60	5,8	235
May	27,4	20,0	12,6	55	7,3	288
Jun	32,8	24,7	16,5	48	13,7	323
Jul	36,9	28,0	19,0	41	20,9	363
Aug	36,5	28,0	19,4	43	19	336
Sep	31,6	24,2	16,9	52	10,3	248
Oct	25,1	19,1	13,0	66	7,8	204
Nov	19,1	13,5	7,8	73	8,4	180
Dec	15,3	10,4	5,5	79	8,1	148
YEAR	25,1	18,2	11,4	60	130,5	2903

84

85 2.1. Urban area sheltered by textile shading devices

86 As a heat mitigation strategy, every year since 2002, the local government and a local commerce
87 association install urban canopy shadings over several commercial streets. The shading devices remain
88 installed between May and October, which represents almost a third of the year. The extent of the
89 urban area sheltered by sunshades was 2.980 m² in 2018, but there is an extension project ongoing
90 (Figure 2). Today, there are urban sun sails in four streets (Figure 2): *Jesus y Maria St*, *Cruz Conde St*,
91 *Gondomar St*, and *Concepcion St*. The first two are limited by buildings facing East and West (yellow).
92 The last two, by buildings facing North and South (blue). From now on, we will refer to these as EW
93 streets and NS streets, respectively.

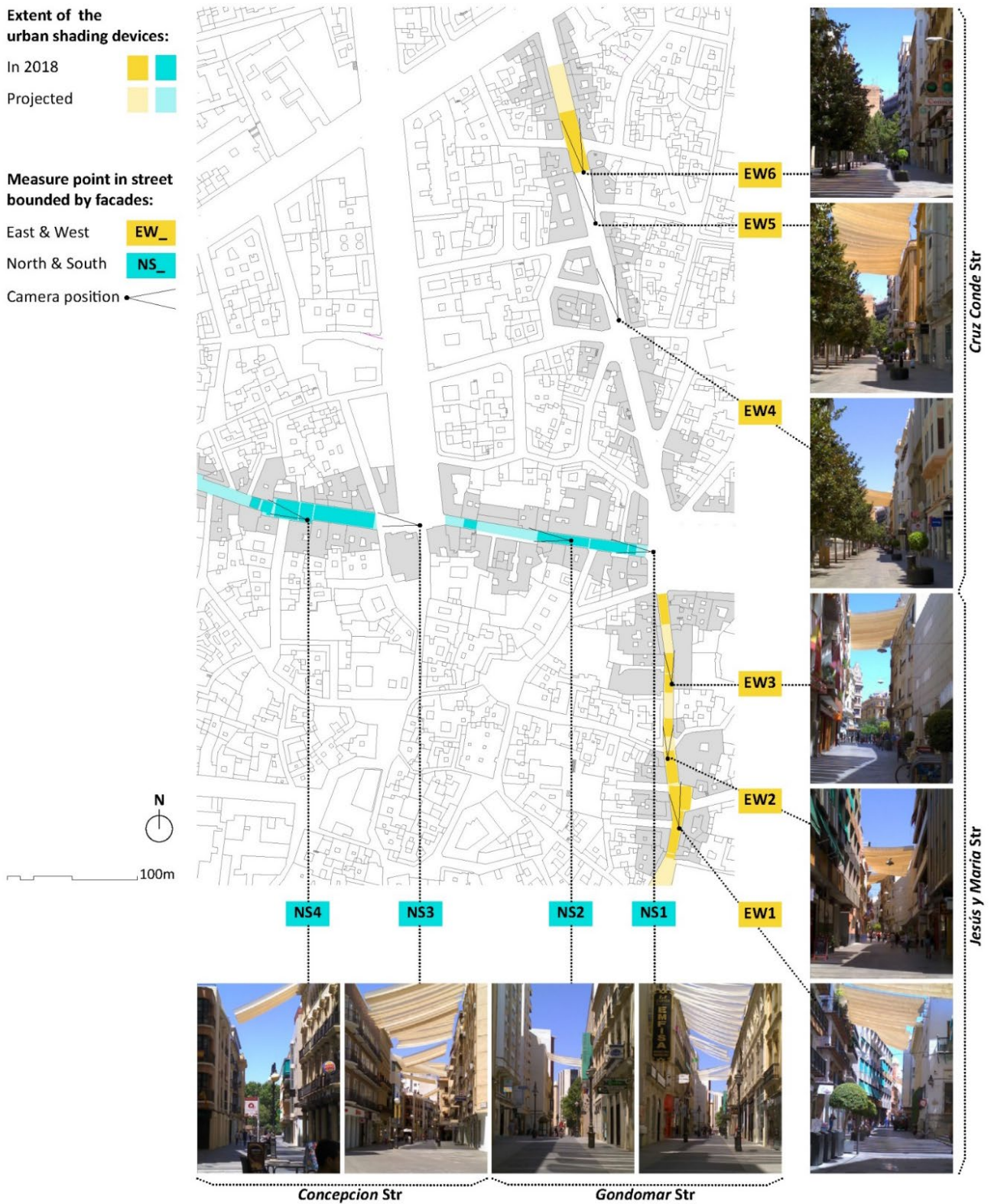
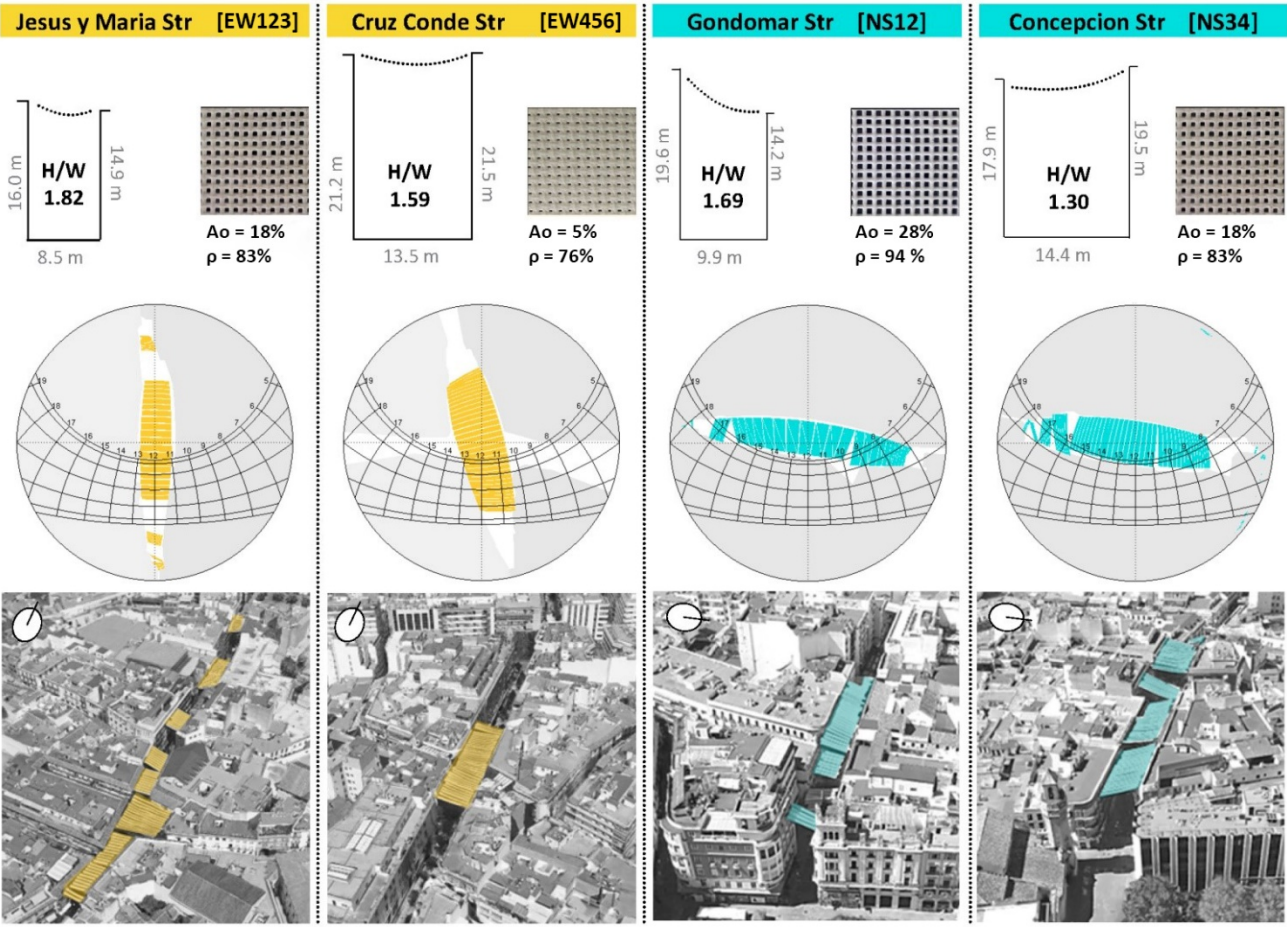


Fig. 2. Urban area sheltered by canopy shading devices in Cordoba, and location of the measurement points for the experimental campaign

98 The selected streets are deep urban canyons with an average aspect ratio ranging between 1.30 and
 99 1.82. Figure 3 depicts stereographic views from the middle of these streets, including solar
 100 obstructions due to both buildings (grey) and shading devices (yellow and blue). In the EW streets
 101 (yellow), urban canopy shadings help to block sunrays impinging on the ground during the central
 102 hours of the day all year long. Conversely, in the NS ones (blue), these devices block the solar radiation
 103 reaching the ground almost all day long for several months around the solstice.



104
 105 Fig. 3. Description of the streets under assessment (from top to bottom): average section, tissue properties, stereographic
 106 view from the middle of the street, perspective aerial view.

107 In Cordoba's city center, all the shading devices are placed on the upper part of the canyon, fixed to
 108 façades through metallic cables with tensors [26]. They consist of a set of rectangular or triangular
 109 pieces of microperforated polyester tissue with an exterior coating of PVC. The length of sails varies
 110 to adapt to the street width, while their width is standard (130 and 260 cm for the rectangular and
 111 triangular ones, respectively). The minimum distance between two adjacent pieces is 20cm, and
 112 between them and the façade plane, 80 cm. This spatial layout and the micro-perforated nature of the

113 tissue allows for diminishing the “sail effect” caused by the wind. This configuration also reduces the
114 stagnation of warm air underneath the shading device, released through the top of the canyon by
115 buoyancy.

116 The properties of textile shading devices differ among the four streets. Figure 3 summarizes their main
117 features. Textile meshes in this urban area present three openness factors (A_o): 5%, 18% and 28%. This
118 parameter plays a key role in textile solar protections since it correlates to the direct normal
119 transmittance of the tissue [27]. Originally white, sun sails presented different hue colors at the time
120 of the measurement campaign, depending on their time of use. This color change in the tissues affects
121 their reflectance (ρ), ranging between 76% and 94%.

122 3. Methods

123 3.1. On site measurements

124 To assess the thermal effects of urban canopy shadings, we carried out a measurement campaign in
125 the zone of Cordoba center sheltered by this kind of device. The core of the experimental work
126 consisted of the shot of a set of visible and infrared images. We conceived this fieldwork to comply
127 with two conditions. First, the work should be feasible counting on limited human and technical
128 resources, corresponding to typical conditions in the pre-diagnosis stage of urban projects. In our case,
129 this stands for: a person operating one commercial thermal camera for one day. The second condition
130 was that a single campaign should be enough to cover all the studied area.

131 To this end, we defined ten measurement points distributed along the four street canyons under
132 assessment (Figure 2). Three criteria guided the location choice: the distance between the
133 measurement points, the representativeness of the framed scene, and the feasibility of the
134 measurement. At each selected location, we placed a FLIR T460 infrared camera (240x320px,
135 FOV=19°x25°) aligned to the street axis with a 10° tilt to the horizontal. This camera position allows
136 for providing a global view of the street, simultaneously framing both facades of the canyon, the
137 pavement, and a fraction of the sky partially blocked by the sun sails. To ensure the repeatability of
138 the shot, we mark the exact position of the camera tripod at each measurement point, as explained in
139 [24].

140 We carried out measurements nine times a day, visiting the selected locations in the same order (from
141 EW1 to NS4). The measurement times were distributed throughout the day to provide a
142 representative view of the thermal behavior of street surfaces throughout the daily cycle. The first
143 round took place one hour before dawn, seeking for a quasi-steady state of street surfaces. The last
144 one, two hours after sunset to capture the effects of inertia. The rest of the rounds were scheduled
145 symmetrically around midday, with smaller intervals in the central hours of the day. Since
146 measurement rounds lasted approximately 40 minutes, each round started 20 minutes before the
147 target hour to minimize the deviation between it and the actual measurement time.

148 Additionally, we collected data on several environmental parameters for the calibration of
149 thermographies and the interpretation of results. The air temperature and the humidity were
150 registered at the pedestrian level using a HOBO thermo-hygrometer. The wind speed was measured
151 with a TESTO i405 hot-wire anemometer at a 2.2-meter height over the street pavement. Global
152 horizontal irradiances (LW and SW) were retrieved from the closest weather station to the
153 experimental site, located at the Cordoba airport.

154 3.2. Image post-processing

155 To obtain graphical material for thermal analysis, we undertook several post-processing tasks on the
156 raw thermographies.

157 First, we calibrated thermographies using the commercial software of the thermal camera (FlirTools+).
158 Air temperature and relative humidity were set to the values recorded during the measurement
159 campaign at the time of each shot. For all the thermographies, the object emissivity was fixed at one
160 and its distance to the camera at zero. Under these conditions, all the objects in the scene are
161 considered black bodies, and the atmosphere is assumed to be completely transparent to the infrared
162 radiation [28]. Thus, the observed temperatures correspond to the “apparent temperatures” deduced
163 directly from the total radiant power reaching the lens in the camera spectral range (7–13 μm).

164 Second, the thermal and visible images taken at each measurement point were registered using
165 automatic intensity-based algorithms (Matlab routine). These images were cropped to the same size
166 to ensure the coherence of the sequence. Though this operation inevitably results in information loss,
167 it can be limited if the camera position is carefully marked. (Notice that the images in this work contain
168 between 93 and 98% of pixels of the raw images). Then, thermal images at each measurement point
169 were ‘stacked’ in chronological order to generate an n-dimension matrix (*multidimensional array*) that
170 allows for reading the thermal dataset in time and space.

171 Finally, we use this thermal dataset to generate the graphical material for analysis. On the one hand,
172 sequences of thermal images with color scales adapted to the phenomena under study. On the other,
173 graphs on the temperature evolution at a certain point of interest.

174 *3.1. Urban modeling and complementary solar analysis*

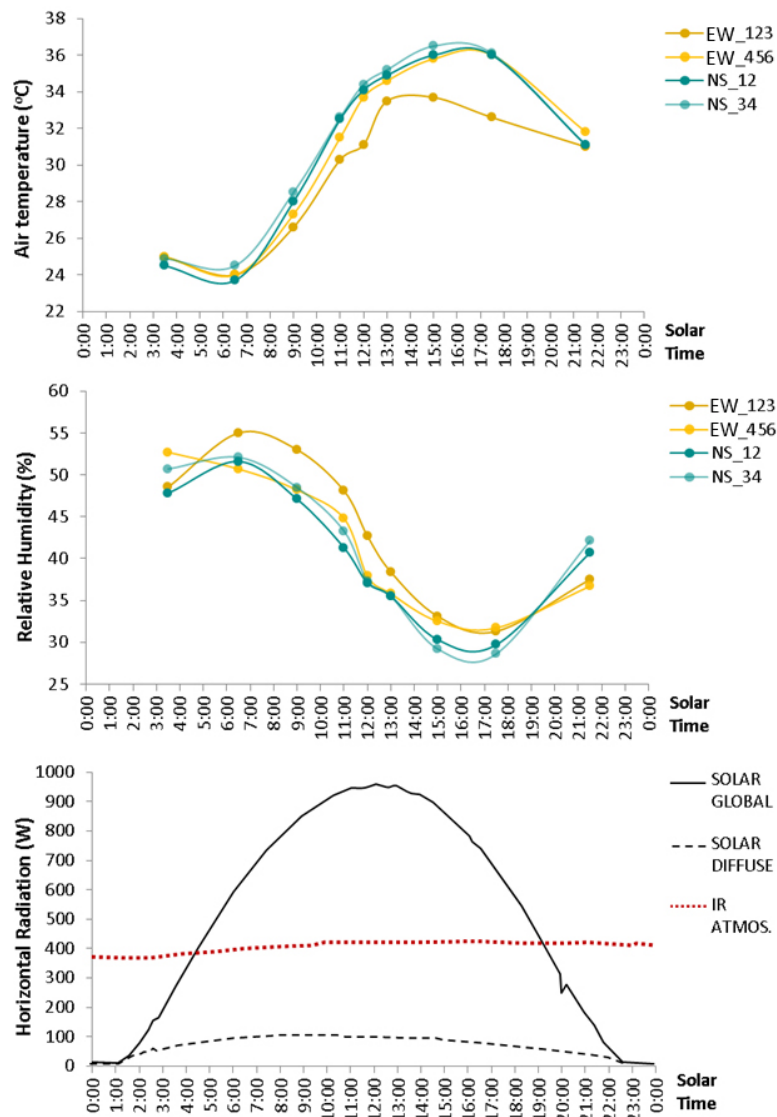
175 To help to understand the experimental results, we carried out complementary solar analyses on a 3D
176 model of the studied urban area. Buildings were modeled by extrusion of the footprints from the
177 cadastral plans, using the information about buildings height gathered from Google Earth Pro. Sun
178 sails were modeled as individual planar surfaces with variable tilt and dimension. The number of pieces
179 and their position were defined according to the technical paper developed by the city council [26].

180 Using the software *Heliodon 2*, we developed two kinds of solar analyses: i) solar exposure studies at
181 certain points of interest based on solar stereographic diagrams; ii) computations of the solar radiation
182 received by urban surfaces through the complete warm season in Cordoba. Notice that *Heliodon 2*
183 computes the solar flux just taking into account the direct component of solar radiation and assuming
184 clear sky conditions [29].

185 4. Results and discussion

186 4.1. Weather conditions

187 Results of the measurements presented here correspond to 8 July 2018, a typical summer day in
188 Cordoba, with a clear sky and warm air temperatures (Figure 4). Air temperatures (T_a) within the four
189 studied streets ranged between 23.7°C (at 06:30h) and 36.5°C (at 17:30h). Minimum air temperatures
190 were similar in the four canyons. Maximum air temperatures, however, exhibited higher differences.
191 The shallowest canyon (Concepcion St) registered the highest air temperatures. Conversely, the
192 narrowest and the most sheltered one (Jesus y Maria St) had the lowest maximum temperatures.



193
194 Fig. 4. Air temperature (up) and relative humidity (middle) within the streets under assessment; Solar and infrared
195 horizontal radiation at Cordoba Airport (down).

196 Atmospheric conditions during the measurement day were dry and calm, which facilitates the
197 thermography interpretation. Relative humidity (RH) in the measurement sites varied between 29%
198 and 55% during the investigated period, with a daily pattern evolving inversely to that of T_a . At the
199 bottom part of the urban canyons, the average wind speed oscillated between 0.1 m/s and 1.6 m/s,
200 remaining most of the times below 1 m/s, a reference value expressed in the literature for
201 thermographic analysis [30].

202 Figure 4 depicts the horizontal short and longwave radiation measured at the Airport weather station
203 on the day of the experimental campaign. These values may be a good approximation of the ones in
204 the study area, given the clear weather conditions and the proximity between these two locations.
205 Solar radiation data corresponded to a typical summer day for the region, with a clear sky and high
206 radiation. The horizontal shortwave global irradiance reached 950 W/m^2 during the central hours of
207 the day, mostly due to direct solar radiation. As for longwave radiation, the sky vault sent an average
208 flux of 400 W/m^2 .

209 *4.2. Temporal and spatial evolution of the sun sails shadows depending on street orientation.*

210 Sun sails unevenly affect the street thermal environment depending on street orientation. To illustrate
211 differences in this regard, Figure 5 presents an excerpt from the image sequence obtained in two
212 perpendicular streets: *Jesus y Maria St* (EW façades) and *Gondomar St* (NS façades).

213

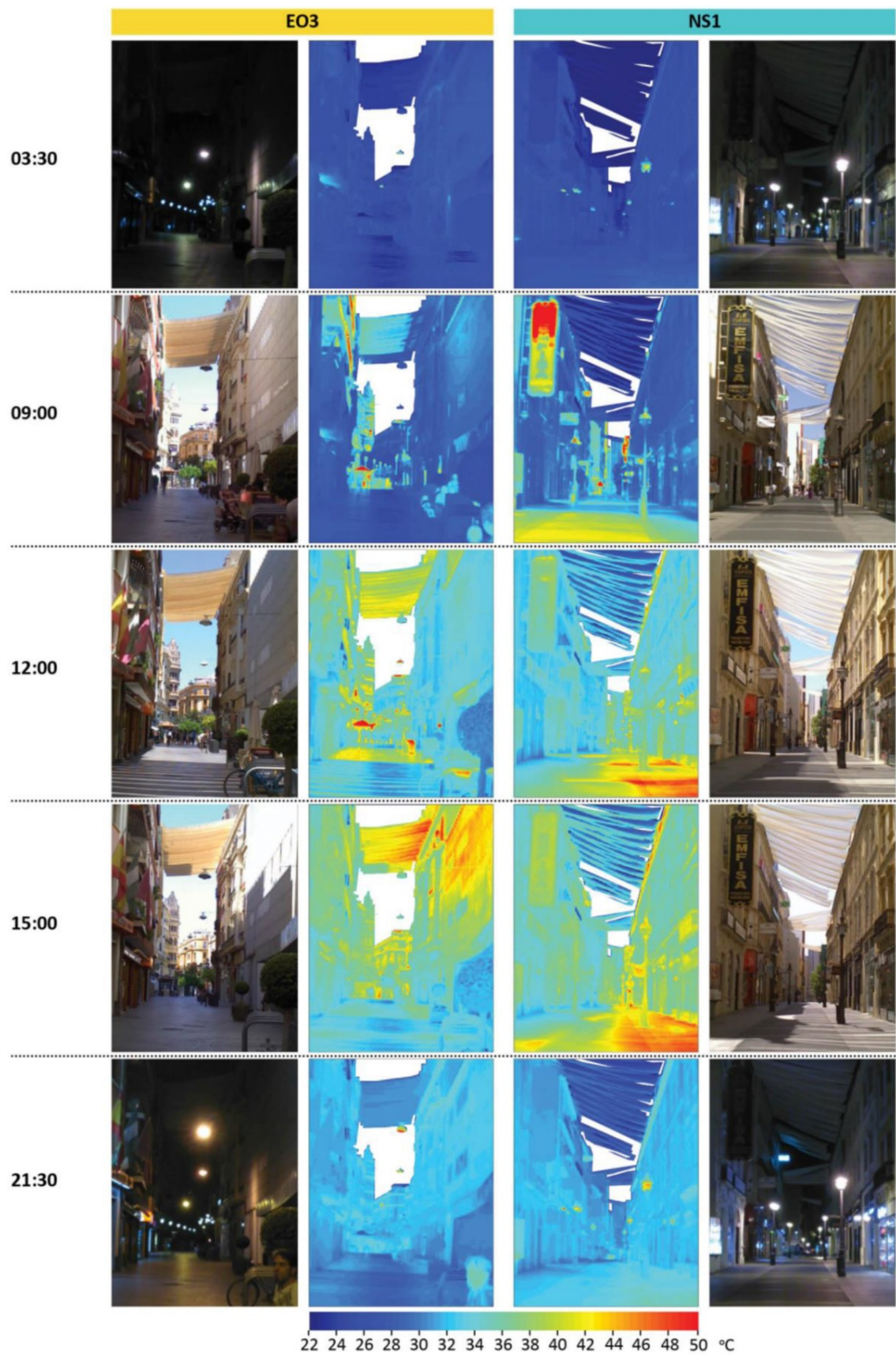


Fig. 5. Excerpt from the visible and infrared time-lapses in Jesus y Maria St (scene EW3, on the left) and Gondomar St (scene NS1, on the right).

217 Results show that, before dawn, surface temperatures were quite homogeneous and close to the air
218 in both urban canyons. At 03:30 ST, temperatures of built surfaces in all the studied urban scenes
219 ranged between 24°C and 29°C, for air temperatures between 24.5°C and 25.0°C. At this time, thermal
220 differences due to the presence of the shading device were small and, consequently, hardly visible
221 when using the suitable color bar for studying the entire day (between 22 and 50°C). Still, it is possible
222 to see that the areas of pavement and façade covered by sun sails in *Gondomar St* were slightly warmer
223 than those with a higher sky view (up to 2°C).

224 After sunrise, the thermal differences among the urban scenes become more evident, due to the
225 uneven solar energy distribution over urban surfaces between orientations. In the same vein, the
226 effects of sun sails are more remarkable during the daytime, generating shaded areas that remain
227 colder than the adjacent sunlit ones. The location and size of these areas depend on the street
228 orientation and the time of the day.

229 During the early hours of summer days, sun sails within streets bounded by East-West façades (such
230 as *Jesus y Maria St*) cast their shadow over the upper part of the East façades. Throughout the
231 morning, the shaded area grows towards the bottom of the canyon, reaching the street pavement
232 only for some hours around noon. At midday, sun sails shade the façade areas below them completely.
233 As the afternoon goes by, the shaded area over the West façade decreases bottom-up. The image
234 time-lapse shows that the shadow of sun sails in streets with East-West façades only affects surfaces
235 placed right below it. Consequently, installing sun sails in these streets allows for creating a 'street
236 section' that remains shaded all day long by either the buildings or the sun sails.

237 Within streets limited by North-South facing façades (such as *Gondomar St*), sun sails shadows present
238 a more dynamic behavior, being able to affect surfaces located far away from the shading device.
239 During the first and last hours of summer days, sun rays penetrate through the ends of the streets,
240 impinging tangentially to both facades (light-colored), and more perpendicularly to the ground (darkly
241 paved). For much of the day (i.e., images at 12:00 and 15:00), sun sails cast shadows on the South
242 façade and the pavement area close to it. All-day long, the cooling effect in this street is more

243 significant over the pavement (darker and receiving more radiation) than over façades (more reflective
244 and less irradiated.

245 Finally, after sunset, surfaces begin to cool down, gradually approaching the air temperature
246 regardless of the street orientation. At 09:30 ST, roughly two hours after sunset, differences between
247 air and built surface temperatures in the studied urban scenes were less than 6°C (between $T_a+3.6$
248 and $T_a-5.4^\circ\text{C}$). The pavement area closer to the base of the South façade of *Gondomar St*, and the
249 upper part of the *Jesus y Maria St* West façade, were the warmest areas of the studied urban canyons,
250 reflecting the inertial effects on surfaces sunlit some hours before.

251 The thermography time-lapses show that sun sails are an effective heat mitigation strategy for both
252 street orientations. However, the surfaces most affected by this cooling effect differ between the
253 cases. Within streets limited by North-South façades, sun sails are especially useful in reducing the
254 ground overheating for much of the day. This effect may be highly beneficial for pedestrian comfort.
255 On the contrary, sun sails over streets perpendicularly oriented are particularly helpful in shading the
256 upper part of street façades in the morning and afternoon. These solar and thermal loads are critical
257 regarding indoor comfort and cooling energy demand. Consequently, sun sails installed in this
258 orientation are especially beneficial for building users, especially those in the higher floors, as
259 investigated in [31].

260 Figures 6 and 7 depict the average solar radiation received over the ground and façades of *Jesus y*
261 *Maria St* and *Gondomar St* between 15 May and 15 September, with and without sun sails. According
262 to simulations, radiation patterns for this period are similar to the ones obtained for the measurement
263 day (8 July). Therefore, remarks about the spatial effects of sun sails in this work are essentially valid
264 for the complete warm season in Cordoba.

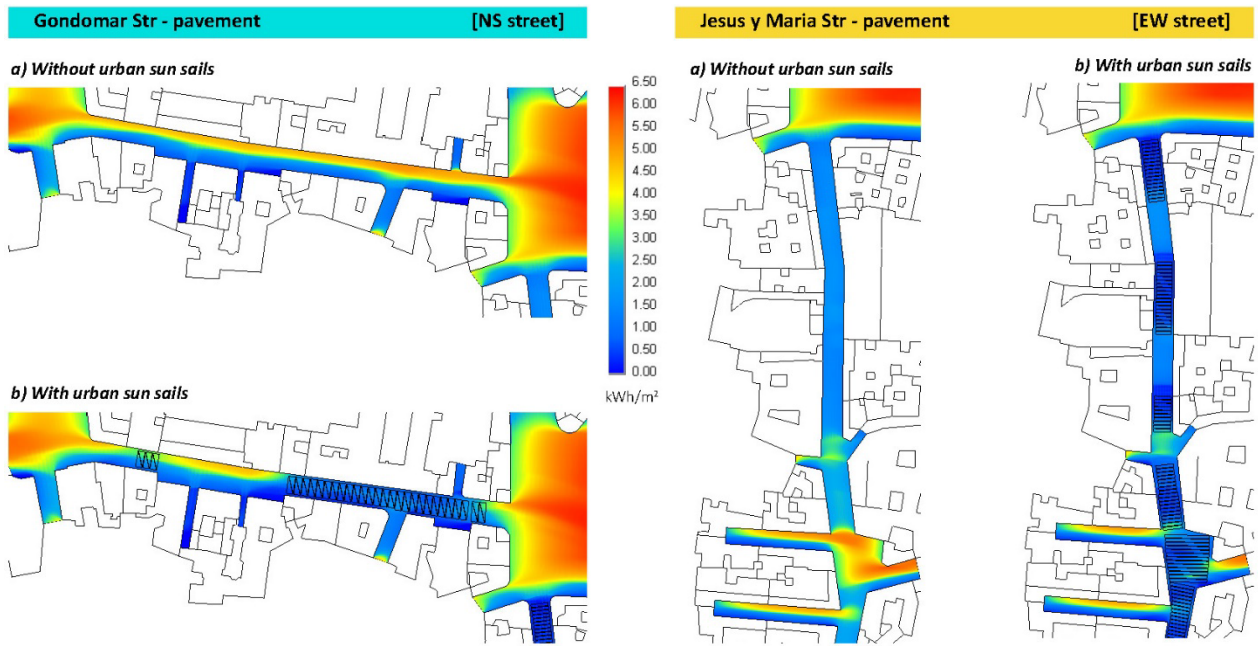


Fig. 6. Direct solar radiation impinging over the pavement of Gondomar St (left) and Jesus y Maria St (right) between 15 May and 15 September, with and without urban canopy shadings.

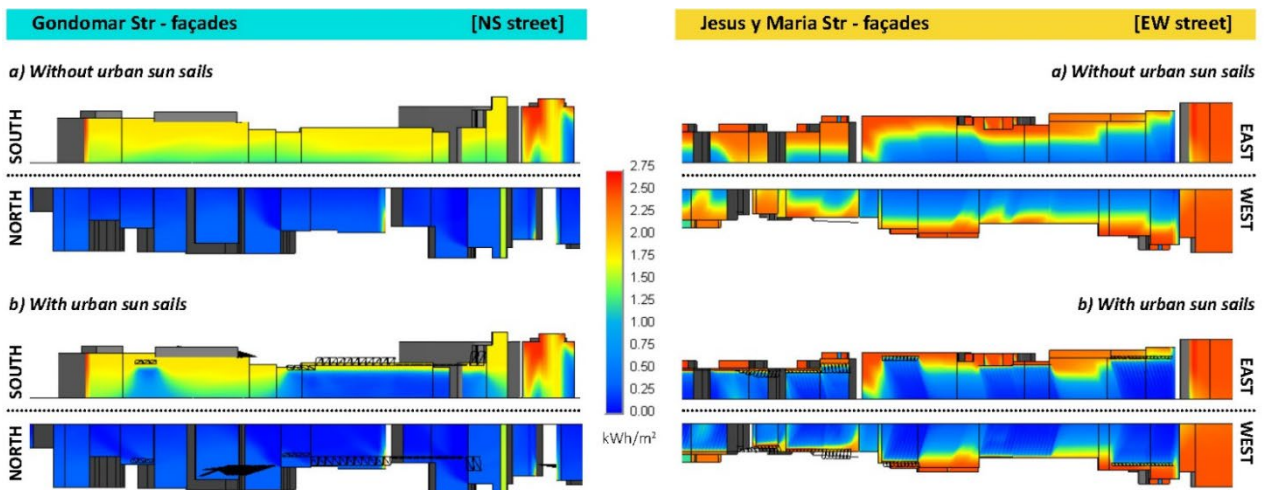
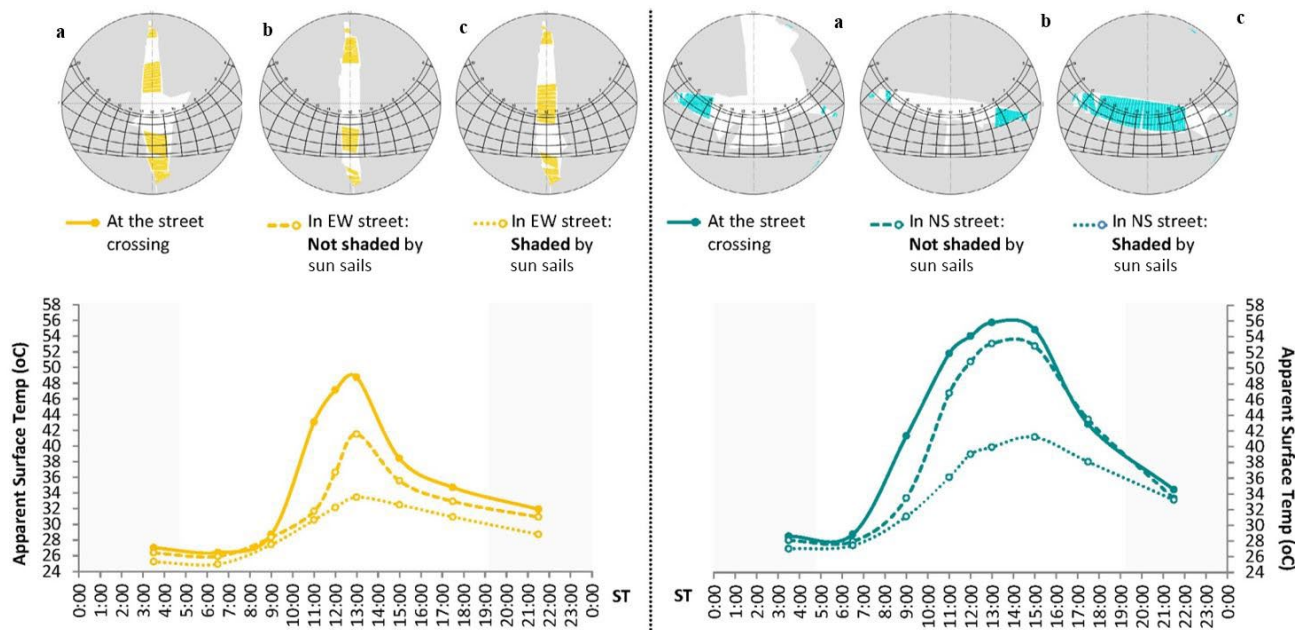


Fig. 7. Direct solar radiation impinging over the façades of Gondomar St (left) and Jesus y Maria St (right) between 15 May and 15 September, with and without opaque sun sails.

273 **4.3. Impact of urban sunshades over urban canyon surface temperatures.**

274 This section analyzes the impact of urban sun sails on the temperatures of the main street surfaces:
275 pavement and façades. Results show that the reduction in surface temperature due to sun sails is
276 more significant over the former than the latter. The overlap of two different factors explains this
277 behavior. First, horizontal surfaces are the ones receiving the maximal irradiance during summer (up
278 to 950 W/m²). Second, in the investigated urban scenes, ground surfaces are generally darker than
279 façades, hence having a higher solar absorptance on average.

280 To investigate the cooling effect of sun sails over the ground, we selected three regions of interest on
281 the pavement with different levels of solar exposure (Figure 8): at the street intersections (a), within
282 the street but not shaded by sun sails (b), within the street and shaded by them all day long (c).



283
284 *Fig. 8. Stereographic diagrams and apparent surface temperature of pavement areas in NS and EW streets*
285 *(blue and yellow, respectively) with different levels of solar exposure (a,b,c).*

286 The results show that the pavement zones shaded by the urban sun sails (c) were cooler than the other
287 two situations assessed (a & b) all day long and for both street orientations. The cooling effect of sun
288 sails over the pavement was maximal one hour after midday (moment of maximum horizontal
289 irradiance). The differences between the cases gradually decreased throughout the afternoon, but
290 they were still perceptible at the early hours of the day (up to 1.8°C until 06:30 ST). These results
291 indicate that the cooling effect of sun sails over the pavement was more noticeable and lasted longer

292 in the NS streets (up to 15.9°C) than in the EW ones (up to 13.2°C). Notice, though, that the pavement
 293 area receiving direct solar radiation in NS streets consists of a 'strip' close to the South façades, whose
 294 width depends on the street aspect ratio. Therefore, sun sail benefits over the ground may affect a
 295 small area or even disappear in deep NS streets. On the contrary, these benefits will exist on the
 296 pavement of EW streets regardless of their aspect ratio, but lasting for a short period in deep canyons.
 297 Unlike the ground, façades in this urban area are quite heterogeneous. This diversity in the optical and
 298 thermal properties of surfaces leads to significant temperature differences between adjacent zones
 299 of the same façade. Generally, the sun sail cooling potential over façades will be higher on those with
 300 high solar absorptance and highly irradiated. Within the urban context, these latter correspond to the
 301 less obstructed parts of East and West façades. Therefore, we focus the discussion about the sun sail
 302 cooling potential over façades on an EW street (*Jesus y Maria St*). We studied in further detail the four-
 303 story building indicated in Figure 9. The choice of this building is of especial interest since it has an
 304 almost homogeneous façade made of concrete slabs ($\alpha=0.5$; $\varepsilon=0.90$), half-sheltered by sun sails.



305
 306 *Fig. 9. Points of interest building for the study of the sun sail thermal effect over façades (dashed line).*

307 Figure 10 depicts the evolution of surface temperatures throughout the day in two adjacent regions
 308 of the façade with the same area: 'b' is sheltered by sun sails, and 'a' is exposed to the sky and receiving
 309 direct solar radiation during the afternoon.

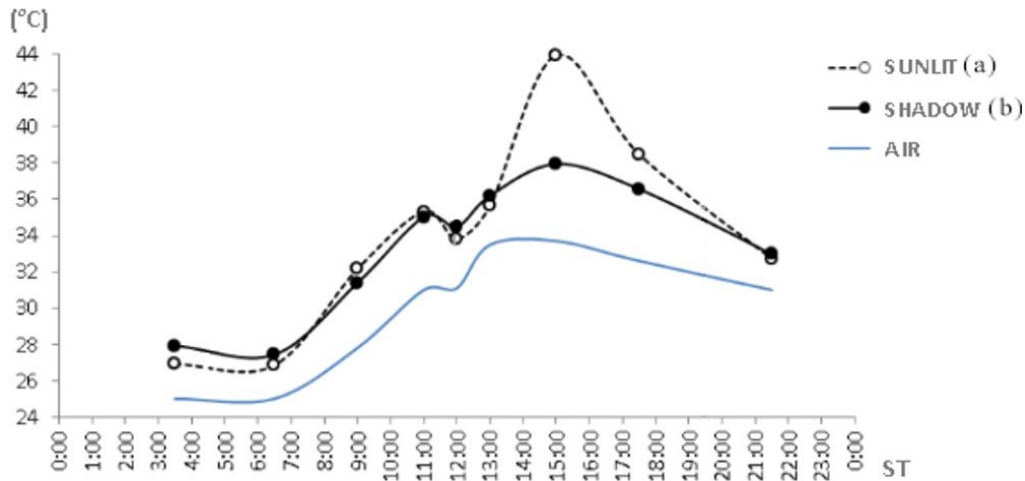


Fig. 10. Comparison between the surface temperature of a shaded (b) and sunlit (a) region of a West façade in Jesus y Maria St.

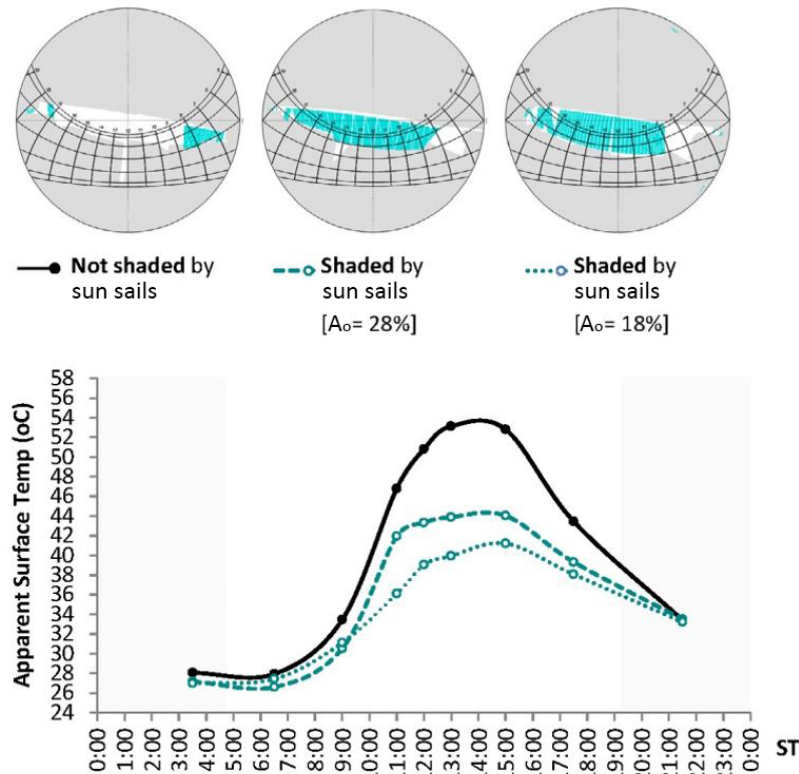
The results show that both regions registered the highest temperatures around 15:00 ST, the time of the day when the façade was receiving the maximum of direct radiation. At that moment, the sunlit region (a) was 6°C warmer than the one shaded by sun sails (b). The thermography in Figure 9 shows a similar cooling effect over all the façade area shaded by sun sails. Additionally, this thermal image evidences that sun sails heat up to some extent, becoming a new heat source for street surfaces.

During the rest of the day, thermal differences between the regions 'a' and 'b' were more limited. Façade areas under the shading device were slightly warmer than the ones outside it at several times of the measurement day. The maximal differential in this sense occurred at dawn when the sheltered region was 1°C warmer than the exposed one.

4.4. Influence of tissue features on the street thermal environment

In this section, we compare the thermal behavior of *Gondomar St* and *Concepcion St* to address the impact of the sun sail features on the street thermal environment. The selected streets are geometrically similar in terms of orientation and cross-section. However, they differ in the characteristics of the urban solar protections, being lighter-colored and more perforated in *Gondomar St* than in *Concepcion St* (Figure 3). Results show that the differences in the optical properties of the tissues resulted in temperature differences between the urban scenes, concerning both built surfaces and sun sails.

330 To analyze the influence of tissue properties on surface temperature, we focused on the ground of
 331 both streets. To this end, we compared the surface temperatures in three pavement zones with the
 332 same finishing (granite slabs: $\rho=0.2$ and $\epsilon=0.96$) but different shade conditions (Figure 11).

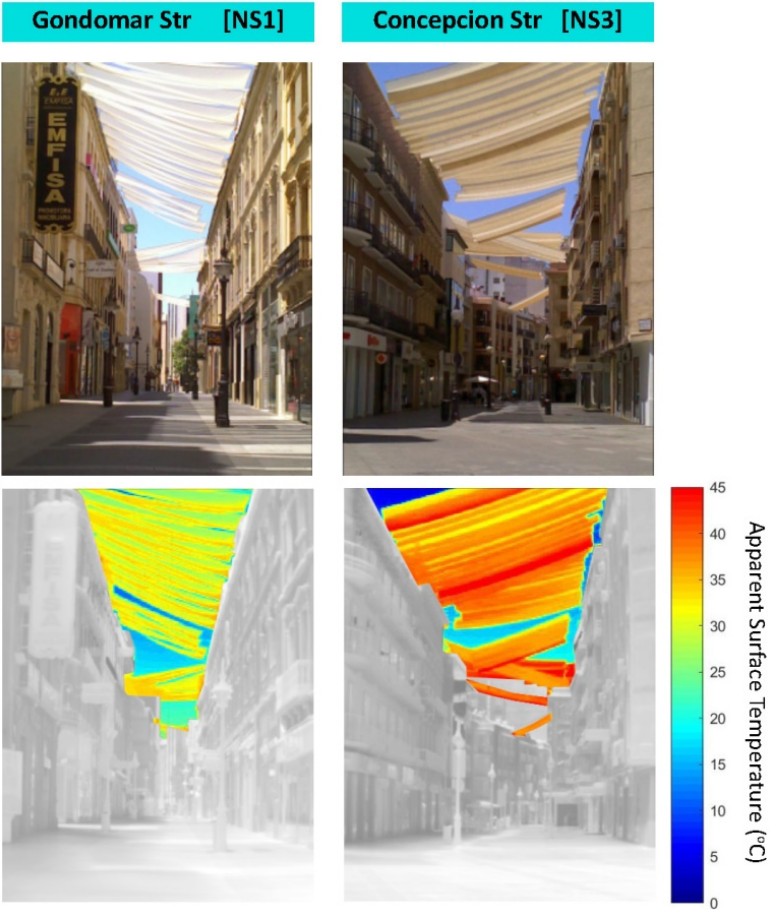


333

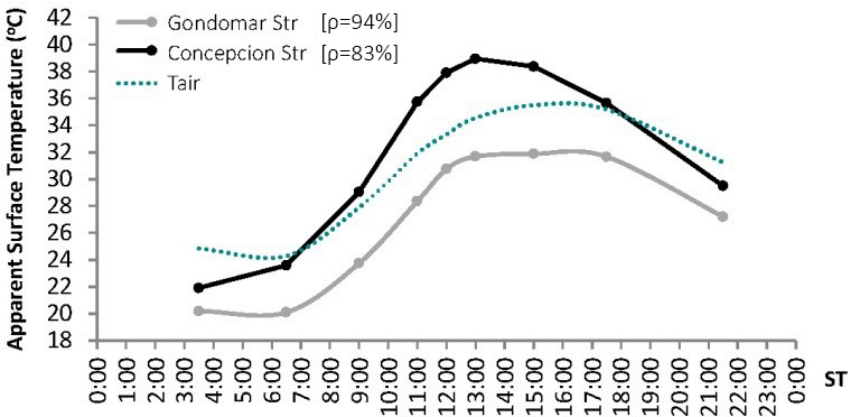
334 *Fig. 11. Surface temperature of pavement areas: sunlit vs shaded by sun sails with different openness factors (A_o).*

335 These results show that the two pavement zones protected by the urban shading devices remained
 336 cooler than the one not shaded by them. However, the intensity of this cooling effect differed between
 337 the streets: up to -13.2°C in Concepcion St, up to -9.2°C in Gondomar St. The difference in tissue
 338 openness may explain this variation: the higher the openness of the tissue is, the lower the cooling
 339 potential of the sun sail. This correlation, though, seems to be not linear since increasing the openness
 340 factor by 10% points reduced the cooling effect by 30%. This behavior may be due to the influence of
 341 this parameter not only on the solar radiation directly impinging on street surfaces but also by
 342 reflection. These findings highlight the key role of tissue openness since relatively small changes in this
 343 parameter result in significant temperature variations. Though the tissue openness should be as low
 344 as possible to maximize sun sail benefits, an excessively low value of this parameter can generate an
 345 unpleasant 'indoor sensation'. Paolini et al. [18] suggest a minimum openness of 10% to avoid this
 346 effect.

347 Finally, we analyze the influence of the tissue reflectance on the temperature of the shading devices
 348 themselves. To this end, we compare the thermal behavior of the sun sails installed in *Gondomar St*
 349 and *Concepcion St* (Figure 12). Graphs in Figure 13 correspond to the average apparent temperatures
 350 of the image region corresponding to sun sails in the thermography time-lapses shot in these streets.



351
 352 Fig. 12. Photography and thermography of sun sails with different reflectance in:
 353 Gondomar St ($\rho=94\%$) and Concepcion St ($\rho=83\%$) at 12:00.



354
 355 Fig. 13. Average apparent surface temperatures of sun sails with different reflectance in:
 356 Gondomar St ($\rho=94\%$) and Concepcion St ($\rho=83\%$) at 12:00.

357 During the measurement campaign, sun sails in Concepcion St were warmer than in Gondomar St,
358 with differences ranging between 1.7°C and 7.4°C. This behavior seems to correlate to the difference
359 in the tissue reflectance between the two cases: the higher the reflectance of the tissue, the lower its
360 apparent temperature. Notice that a relatively small difference in the tissue reflectance (11 %points)
361 led to a significant change in its apparent temperature (up to 7.4°C).

362 Textile shading devices are thin and lightweight elements with a low thermal capacity. Consequently,
363 their heat storage is almost negligible, and convective and radiative fluxes will mainly drive their
364 surface temperature. Under clear sky conditions, sun sails will be substantially warmer than the sky
365 vault regardless of the tissue color (Figure 12). When made of light-colored tissues, sun sails
366 temperatures remain similar to the surrounding air all day long (Figure 13). Low-reflective tissues, in
367 contrast, may significantly overheat, becoming an additional heat source for pedestrian and built
368 surfaces. Longwave exchanges with shading devices may have a noticeable impact on urban comfort
369 [19] and cooling demand [32]. Therefore, to maximize benefits from sun sails on human comfort and
370 energy consumption, tissues with high reflectance and low transmittance are preferable.

371 5. Discussion

372 Results show that sun sails allow for significant reductions in the daytime temperatures of urban
373 surfaces. This cooling is due to the prime benefit of these devices: a reduction in the shortwave
374 radiation absorbed by street surfaces. Sun sails have, though, some adverse effects on the street
375 microclimate that partially offset the temperature lowering achieved due to shading:

- 376 • **A reduction in the radiative cooling of urban surfaces towards the sky.** Our results show that,
377 due to this effect, surfaces below sun sails are slightly warmer during the night than those
378 adjacent but more exposed to the sky (up to 2°C). This rise in temperature, though small, might
379 have some impact on the quality of outdoor and indoor climates. In this regard, Evins et al. [32]
380 showed that small changes in the outside building temperature (+2°C, on average) could
381 significantly affect building cooling demands (+19%). Further investigations are required to
382 assess the convenience of installing night-removable shading devices.
- 383 • **A reduction of the wind speed within the canyon.** In the investigated case study, the use of sun
384 sails seems to have a minor impact on wind speed, since wind conditions in Cordoba are
385 already calm without these devices. As sun sails overheat when sunlit, they could foster an
386 upward movement of warm air that could partially counterbalance the absence of wind. Given
387 the crucial role of wind speed for urban comfort and thermal building performance, it would
388 be advisable case-by-case analyses in this regard.

389 Onsite observations are invaluable since only they represent the real complexity of the problem under
390 investigation. Besides, measurements provide useful insights and data to compare with simulations
391 models, that could extend their usefulness [1]. Our experimental data are in good agreement with
392 simulations in [18], which show temperature decreases over the pavement of up to 12°C for a street
393 in Milan with similar climatic and material conditions to the ones in Cordoba. In contrast, we found
394 significant differences when comparing to other theoretical works, such as [6]. This work found higher
395 decreases in surface temperature due to the use of sun sails (up to 27°C on the pavement), despite
396 considering a less opaque tissue. The discrepancies between the simulated and measured studies
397 highlight the need for field data on the cooling potential of sun sails in real urban environments.

398 6. Conclusions

399 This paper presents an empirical study on the impact of urban sun sails on street surface temperatures.
400 The work relies on the results of a thermographic campaign conducted in four streets of the historical
401 center of Cordoba sheltered by these devices. Based on the field observations, we draw the following
402 conclusions about:

403 • **The potential of sun sails as heat mitigation strategy at a street scale.** During the day, the use of
404 sun sails significantly limited the overheating of the urban surfaces, especially of the dark and
405 highly irradiated ones. Thus, the most intense cooling effect of sun sails in this case study
406 occurred over the pavement, reducing its temperature up to 16°C. The decrease in façade
407 temperatures was also noticeable, reaching 6°C on walls with a mid-reflectance. These results
408 demonstrate that sun sails allow for a surface temperature lowering similar to standard
409 mitigation technologies (e.g., cool coatings [33,34]), while entailing softer levels of intervention
410 on the built environment. During the night, surfaces below sun sails were slightly warmer than
411 those more exposed to the sky (<2°C). Future works should assess the benefits of installing
412 removable-devices to counteract this effect.

413 • **Guidelines for the installation of street sun sails.** Installing high-mounted devices is
414 crucial to ensure that sun sails have a global cooling effect over the street. Sun sails should
415 have the lowest possible solar transmittance and the highest possible reflectance to maximize
416 their benefits. Thus, the tissue openness should be as low as possible (though not below 10%
417 to avoid an 'indoor sensation'). In our case study, an increase in the tissue openness of 10
418 points (from 18% to 28%) reduced the cooling effect of sun sails by 30% (from -13.2°C to -
419 9.2°C). Also, light-colored tissues are preferable to limit sun sail overheating. Sun sails are
420 highly effective in reducing surface temperature regardless of street orientation. In streets with
421 Nord-South façades, sun sails are especially beneficial in lowering pavement temperatures,

crucial for pedestrian comfort. In those with East-West façades, the main benefits of sun sails concern the building façades, thus building users.

- **The potential of perspective time-lapse thermography for microclimate studies.** Street-based thermography has only been used occasionally in urban climate research, thus, a major contribution of this work was to the advancement of the observational technique. The use of perspective views demonstrated to be an agile way for acquiring a global thermal information at street scale, even counting on limited resources (one person, one camera, one day).

To our knowledge, this study is the first experimental work about the potential of sun sails as a heat mitigation technology relying on street-based thermography. In this sense, our observations contribute to a better understanding of urban climate in two ways: from the methodological point of view, by presenting a novel approach that might help to address the gap in microclimate data at the street level; and, from a climate-conscious design perspective, by highlighting sun sails as a highly effective soft intervention.

437 **Acknowledgements**

438 This work was supported by the Spanish Ministry of Education [grant number FPU-13/0388], the
439 Region of Nouvelle Aquitaine and the Urban Agglomeration of Côte Basque Adour.

440 **References**

- 441 [1] T.R. Oke, G. Mills, A. Christen, J.A. Voogt, Urban Climates, Cambridge University Press,
442 Columbia, 2017.
- 443 [2] C. Smith, G. Levermore, Designing urban spaces and buildings to improve sustainability and
444 quality of life in a warmer world, *Energy Policy*. 36 (2008) 4558–4562.
- 445 [3] F. Lindberg, S. Thorsson, D. Rayner, K. Lau, The impact of urban planning strategies on heat
446 stress in a climate-change perspective, *Sustain. Cities Soc.* 25 (2016) 1–12.
- 447 [4] B.A. Norton, A.M. Coutts, S.J. Livesley, R.J. Harris, A.M. Hunter, N.S.G. Williams, Planning for
448 cooler cities: A framework to prioritise green infrastructure to mitigate high temperatures in
449 urban landscapes, *Landsc. Urban Plan.* 134 (2015) 127–138.
- 450 [5] M. Santamouris, Using cool pavements as a mitigation strategy to fight urban heat island—A
451 review of the actual developments, *Renew. Sustain. Energy Rev.* 26 (2013) 224–240.
- 452 [6] S. Saneinejad, P. Moonen, J. Carmeliet, Comparative assessment of various heat island
453 mitigation measures, *Build. Environ.* 73 (2014) 162–170.
- 454 [7] M. Santamouris, L. Ding, F. Fiorito, P. Oldfield, P. Osmond, R. Paolini, D. Prasad, A. Synnefa,
455 Passive and active cooling for the outdoor built environment – Analysis and assessment of the
456 cooling potential of mitigation technologies using performance data from 220 large scale
457 projects, *Sol. Energy*. 154 (2017) 14–33.
- 458 [8] H. Akbari, C. Cartalis, D. Kolokotsa, A. Muscio, A.L. Pisello, F. Rossi, M. Santamouris, A. Synnef,
459 N.H. WONG, M. Zinzi, Local Climate Change and Urban Heat Island Mitigation Techniques – the
460 State of the Art, *J. Civ. Eng. Manag.* 22 (2015) 1–16.

- 461 [9] F. Ali-Toudert, H. Mayer, Numerical study on the effects of aspect ratio and orientation of an
462 urban street canyon on outdoor thermal comfort in hot and dry climate, *Build. Environ.* 41
463 (2006) 94–108. <https://doi.org/10.1016/j.buildenv.2005.01.013>.
- 464 [10] F. Bourbia, F. Boucheriba, Impact of street design on urban microclimate for semi arid climate
465 (Constantine), *Renew. Energy*. 35 (2010) 343–347.
- 466 [11] F. Bourbia, H.B. Awbi, Building cluster and shading in urban canyon for hot dry climate Part 1:
467 Air and surface temperature measurements, *Renew. Energy*. 29 (2004) 249–262.
- 468 [12] H. Akbari, M. Pomerantz, H. Taha, Cool surfaces and shade trees to reduce energy use and
469 improve air quality in urban areas, *Sol. Energy*. 70 (2001) 295–310.
- 470 [13] C.Y. Park, D.K. Lee, E.S. Krayenhoff, H.K. Heo, J.H. Hyun, K. Oh, T.Y. Park, Variations in pedestrian
471 mean radiant temperature based on the spacing and size of street trees, *Sustain. Cities Soc.* 48
472 (2019) 1–9.
- 473 [14] B. Morille, M. Musy, L. Malys, Preliminary study of the impact of urban greenery types on energy
474 consumption of building at a district scale: Academic study on a canyon street in Nantes (France)
475 weather conditions, *Energy Build.* 114 (2016) 275–282.
- 476 [15] N. Kántor, L. Chen, C. V. Gál, Human-biometeorological significance of shading in urban public
477 spaces—Summertime measurements in Pécs, Hungary, *Landsc. Urban Plan.* 170 (2018) 241–
478 255. <https://doi.org/10.1016/j.landurbplan.2017.09.030>.
- 479 [16] R.-L. Hwang, T.-P. Lin, A. Matzarakis, Seasonal effects of urban street shading on long-term
480 outdoor thermal comfort, *Build. Environ.* 46 (2011) 863–870.
- 481 [17] B.L. J. Chilton, Lighting and the visual environment in architectural fabric structures, in: J.I.
482 Llorens (Ed.), *Fabr. Struct. Archit.*, Elsevier - Woodhead Publishing Series in Textiles, 2015: pp.
483 203–219.
- 484 [18] R. Paolini, A.G. Mainini, T. Poli, L. Vercesi, Assessment of Thermal Stress in a Street Canyon in

485 Pedestrian Area with or without Canopy Shading, *Energy Procedia*. 48 (2014) 1570–1575.

486 [19] L. Shashua-Bar, D. Pearlmutter, E. Erell, The influence of trees and grass on outdoor thermal
487 comfort in a hot-arid environment, *Int. J. Climatol.* 31 (2011) 1498–1506.

488 [20] H. Swaid, Intelligent urban forms (IUF) a new climate-concerned, urban planning strategy,
489 *Theor. Appl. Climatol.* 46 (1992) 179–191.

490 [21] J. a. Voogt, T.R. Oke, Complete Urban Surface Temperatures, *J. Appl. Meteorol.* 36 (1997) 1117–
491 1132.

492 [22] K. Fabbri, V. Costanzo, Drone-assisted infrared thermography for calibration of outdoor
493 microclimate simulation models, *Sustain. Cities Soc.* 52 (2020) 101855.

494 [23] F. Meier, D. Scherer, J. Richters, A. Christen, Atmospheric correction of thermal-infrared
495 imagery of the 3D urban environment acquired in oblique viewing geometry, *Atmos. Meas.*
496 *Tech.* 4 (2011) 909–922.

497 [24] E. Garcia-Nevado, Termografía del cañón urbano: uso de la perspectiva para una evaluación
498 térmica global de la calle (PhD Thesis), Universitat Politècnica de Catalunya, 2019.
499 <http://www.tdx.cat/handle/10803/666702> (accessed May 10, 2019).

500 [25] AEMET - Agencia Estatal de Meteorología, Valores climatológicos para el período de referencia
501 1981-2010: Córdoba Aeropuerto, (n.d.).

502 [26] M. Castro del Río, Memoria de Licitación de Proyecto de entoldado de calles del centro de
503 Córdoba 2018, Ayuntamiento de Córdoba - Delegación de Medio Ambiente e Infraestructuras,
504 Córdoba, 2018.

505 [27] N. Kotey, J.L. Wright, M. Collins, Determining off-normal solar optical properties of Roller Blinds,
506 *ASHRAE Trans.* 115 PART 2 (2009) 3–17.

507 [28] T. Kruczek, Use of infrared camera in energy diagnostics of the objects placed in open air space
508 in particular at non-isothermal sky, *Energy*. 91 (2015) 35–47.

- 509 [29] B. Beckers, L. Masset, Heliodon 2. Software and User Guide, (2006). www.heliodon.net.
- 510 [30] M. Vollmer, K.P. Möllmann, Infrared Thermal Imaging. Fundamentals, Research and
511 Applications., Wiley, Weinheim, 2010.
- 512 [31] E. Garcia-Nevado, Toldo urbano: Posibilidades de reducción de la demanda de refrigeración
513 (Master Thesis), Universitat Politècnica de Catalunya (UPC), 2013.
- 514 [32] R. Evins, V. Dorer, J. Carmeliet, Simulating external longwave radiation exchange for buildings,
515 Energy Build. 75 (2014) 472–482.
- 516 [33] M. Santamouris, N. Gaitani, a. Spanou, M. Saliari, K. Giannopoulou, K. Vasilakopoulou, T.
517 Kardomateas, Using cool paving materials to improve microclimate of urban areas – Design
518 realization and results of the flisvos project, Build. Environ. 53 (2012) 128–136.
- 519 [34] C. Georgakis, S. Zoras, M. Santamouris, Studying the effect of “cool” coatings in street urban
520 canyons and its potential as a heat island mitigation technique, Sustain. Cities Soc. 13 (2014)
521 20–31.
- 522